Int. J. Electrochem. Sci., 16 **(2021)** Article ID: 210437, doi: 10.20964/2021.04.34

International Journal of
ELECTROCHEMICAL
SCIENCE
www.electrochemsci.org

A Sensing Interface Based on 3D CS-Au NPs/hPPy for Electrochemical Detection of Carcinoembryonic Antigen

Shangshang Ma[1,2], *Qing Zhang*[1,2*], *Miao Qin*[1,2], *Hongyan Wang*[1,2], *Yanyan Zhu*[1,2], *Yi Zhang*[1,2], *Keying Zhang*[1,2*]

[1] Key Laboratory of Spin Electron and Nanomaterials of Anhui Higher Education Institutes, Suzhou University, Suzhou 234000, People's Republic of China
[2] School of Chemistry and Chemical Engineering, Suzhou University, Suzhou 234000, People's Republic of China
[*]E-mail: qingzhang_ahszu@163.com (Q. Zhang), zhangky1983@163.com (K. Zhang)

Received: 17 December 2020 / *Accepted:* 6 February 2021 / *Published:* 28 February 2021

Carcinoembryonic antigen (CEA), a major tumor marker, has been applied to clinical screening and early diagnosis. Herein, an electrochemical detection platform using three-dimensional horn-like PPy (hPPy) and CS-Au nanoparticles micro/nanostructure as sensing interface, was utilized to detect varied concentrations of CEA. On account of the large specific surface area, remarkable conductivity, stability and biocompatibility of 3D CS-Au NPs/hPPy, low concentration of CEA could be detected precisely. Under optimal conditions of pH, incubation time and temperature, the electrochemical immunosensor showed favorable linear relationship, wide CEA detection scope of 0.01 to 120 ng/mL with a low detection limit of 0.0036 ng/mL (signal-to-noise ratio = 3). Besides, the prepared immunosensor revealed favourable specificity and stability for detection of CEA. Furthermore, such immunosensors applied in determination of CEA in human blood had satisfactory consistency comparing with the detected CEA reference values of hospital, implying that the 3D CS-Au NPs/hPPy sensing interface we obtained have reliability in cancer diagnosis and potential application in clinical immunology.

Keywords: Three-dimensional micro/nanostructure, 3D CS-Au NPs/hPPy, Electrochemical biosensor, CEA

1. INTRODUCTION

Malignant tumor with high mortality is a serious threat to human health[1]. Early diagnosis and intervention of malignant tumor is the key to improve the survival rate of cancer patients[2]. Studies have shown that the occurrence of malignent tumors is closely associated with gene expression of

related proteins in cells. Therefore, the establishment of a rapid, accurate and sensitive technology for detecting marked proteins of tumor cells is significant for the study of tumor pathogenesis, early diagnosis and treatment[3]. CEA is a major tumor biomarker applied to clinical cancer screening and early diagnosis. The detection of CEA has clinical significance in the diagnosis, disease detection and curative effect assessment of gastric cancer[4], lung cancer[5, 6], colorectal cancer[7], breast cancer[8] and other malignant tumors[9]. Therefore, the rapid and high sensitivity detection methods for CEA have become a research hotspot recently[10-13]. A varity of methods have been reported to determine CEA, including enzyme-linked immunosorbent assay (ELISA)[14], surface plasmon resonance[15], electrochemiluminescence (ECL)[16], chemiluminescence (CL)[17] and so on. Among them, electrochemical biosensors have became popular due to its low-budget, enhanced sensitivity, low detection limit and rapid response[18].

Recently, because of the unique hierarchical structure, the nanomaterials has been introduced into the electrochemical field used for sensing platform, which greatly changes the performance of the original electrochemical technology[19, 20]. The introduction of three-dimensional micro-nano structure into electrochemical biosensor can construct excellent sensing interface. Owing to a superior loading surface area of three-dimensional micro-nano structure, more metal nanoparticles are allowed to be loaded on the interface, which contributes to amplifying current signal and accelerating electron transfer[21, 22]. In addition, the unique three-dimensional micro-nano structure helps to enhance the immobilization capacity of biomolecules[23]. Gold (Au) nanoparticles (NPs) hold broad appeal in electrochemical biosensor due to its high conductivity, remarkable chemical stability, biocompatibility and catalytic activity[24-26]. Polypyrrole (PPy) has been widely used as an electroactive material for electrochemical biosensors due to its excellent conductivity, simple preparation, good biocompatibility and environmental friendliness. In addition, horn-like PPy (hPPy) with micro-nano structure is reported to exhibits better electrochemical performance than planar conventional polypyrrole (cPPy), making it more suitable for the construction of electrochemical biosensors[27, 28].

In view of these advantages of gold and polypyrrole using as electrochemical sensors, in this work, a three-dimensional chitosan (CS)-Au NPs/hPPy electrochemical interface with micro/nano structure was designed and fabricated. The ability of Au NPs and CS adsorbing protein was utilized to load the anti-CEA and CEA on the sensing interface to realize the construction of electrochemical immunosensor. The electrochemical methods, differential pulse voltammetry, was applied for test optimal conditions including pH, incubation time and temperature. Under the optimal conditions, the 3D CS-Au NPs/hPPy electrochemical sensing interface could realize ultimate 0.0036 ng/mL determination of CEA with a linear determination scope of 0.01 to 120 ng/mL. Besides, the 3D CS-Au NPs/hPPy electrochemical biosensor was also applied to detect CEA in human blood samples, which showed reliable consistency with the hospital detection results. All test datas showed that 3D CS-Au NPs/hPPy was an excellent electrochemical material for CEA detection, which indicates that it may have great clinical application prospects.

2. EXPERIMENTS SECTION

2.1. Chemicals and reagents

Carcinoembryonic antigen (CEA), carcinoembryonic monoclonal antibody (anti-CEA) and alpha fetoprotein (AFP) were purchased from Shanghai Yu Bo Biotech Co., Ltd (Shanghai China); Urea (UA), ascorbic acid (AA) and glucose (Glu) were obtained from Sinopharm Chemical Reagent Co., Ltd. Pyrrole (Py) and bovine serum albumin (BSA) were obtained from Aladdin Chemistry Co., Ltd (Shanghai, China); Chloroauric acid ($HAuCl_4$, 98%) was purchased from Energy Chemical Co., Ltd (Shanghai, China); Chitosan (630 KDa), toluene-4-sulfonic acid momohydrate (TsOH) and acetic acid were gained from Sinopharm Chemical Reagent Co., Ltd. The human whole blood and serum samples were obtained from Suzhou municipal hospital. The 0.1 M phosphate buffer solution (PBS, pH 7.0) served as cleaning solution. A $[Fe(CN)^6]^{3-/4-}$ solution, containing 10 mM $K_3Fe(CN)_6$, 10 mM $K_4Fe(CN)_6$, and 0.1 M KCl, was prepared for the measurements. Redistilled water (18.2 MΩ) was applied to all experimental process.

2.2. Apparatus

The CHI 660A electrochemical workstation (Shanghai Chenhua company, China) with three electrode system was applied to finish experiments. The images of scanning electron microscopy (SEM) were gained from JSM-6300 FESEM (JEOL Co., Ltd, Japan).

2.3. Processing of 3D CS-Au NPs/hPPy sensing interface

The 3D CS-Au NPs/hPPy sensing interface was synthesized by two-step eletrochemical deposition. Firstly, the hPPy sensing layer was prepared by dissolving 1 mol toluene-4-sulfonic acid momohydrate (TsOH) in 50 mL water to form a homogeneous and stable solution[28, 29]. After that, 170 uL of Py was rapidly implanted to the TsOH solution. The three electrode system, containing a stainless steel plate as working electrode, a platinum (Pt) electrode and a saturated calomel electrode (SCE), was placed in the solution with the scanning speed of 30 mV/s and working voltage of - 0.4 V ~ + 0.8 V for 3 h. Then, an additional 170 uL Py monomer was added to the solution for reacting 3 h. Moreover, the prepared hPPy film was immersed in a blend solution including 0.5 g/L CS solution (1% acetic acid as solvent) and 250 mg/L $HAuCl_4$ solution with a volume ratio of 1:1[30]. Thereafter, the 3D CS-Au NPs/hPPy composite films were obtained by applying 3 V voltage to the above solution for 3 minutes and then dried at ambient temperature.

2.4. Assembly process of electrochemical immunosensor

Firstly, the 3D CS-Au NPs/hPPy films were cut into 1x1 cm small pieces for assembling electrochemical immunosensor. The property of gold to specifically adsorb protein was used to modify the surface of 3D CS-Au NPs/hPPy composite film with 10 ug/mL anti-CEA. Then the non-specific

sites on the sensing surface were sealed by dropwise adding 1% BSA at room temperature and incubating for 40 minutes, which could block non-specific adsorption. After that, PBS solution was used to rinse the dried material gently for 2 ~ 3 times to remove unbound anti-CEA on the surface. Finally, the modified films was incubated with CEA standard solutions at ambient temperature. The successfully assembled immunosensor was applied to CEA detection in Fig. 1.

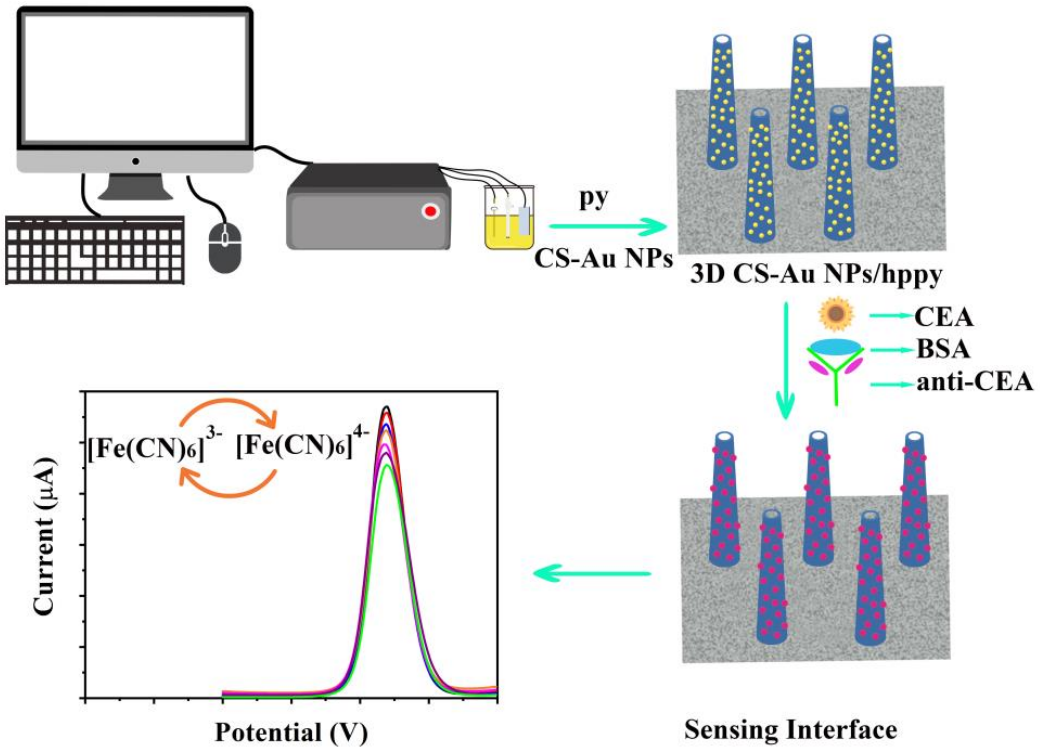

Figure 1. Schematic illustration of the preparation of the 3D CS-Au NPs/hPPy film and sensing for CEA.

2.5. Detection of electrochemical immunosensor

Different concentartions of CEA were united with anti-CEA/3D CS-Au NPs/hPPy. After incubation under the optimal conditions, the materials were rinsed with PBS and secondary water to wiped off the unconjugated CEA. Electrochemical methods including cyclic voltammetry (CV) with scan range from - 0.2 V to + 0.6 V, differential pulse voltammetry (DPV) with scan range from - 0.2 V to + 0.6 V at a pulse frequency of 0.05 V and an amplitude of 50 ms were utilized to finish assessment of electrochemical immunosensor. Apart from that, the EIS Nyquist curves were obtained in 0.1 M PBS (pH = 7.0) electrolyte comprising 10 mM $[Fe(CN)_6]^{3-/4-}$ and 0.1 M KCl in the frequency range of 1 Hz to 100 kHz. The refrigerator temperature was set to 4 ℃ to store the sensors when it was not in use.

3. RESULTS AND DISCUSSION

3.1. Characterization of 3D CS-Au NPs/hPPy film

SEM was applied to assess the structure of 3D CS-Au NPs/hPPy film. Fig. 2A illustrated the SEM image of hPPy film with three dimensional morphology. The Au NPs deposited on hPPy film shown as Fig. 2B. Moreover, the elements C, N, O, Au were characterized by EDS in Fig. 2C, which further demonstrated that the 3D CS-Au NPs/hPPy film was obtained.

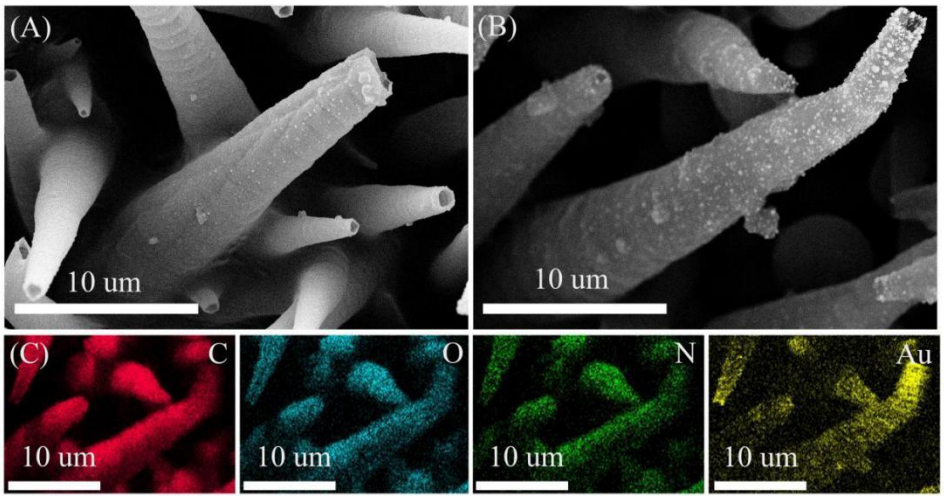

Figure 2. SEM figures of (A) hPPy film; (B) 3D CS-Au NPs/hPPy film and (C) EDS elemental mapping of 3D CS-Au NPs/hPPy, indicating the hPPy film was successfully combined with CS-Au NPs.

3.2. Performance analysis of electrochemical immunosensor

The CV and EIS electrochemical methods were used to record the characteristics of each step to assess the assembly process of immunosensor. The Fig. 3A represented CV diagram of the layer by layer modified immunosensor, which was used to characterize the construction process of immunosersor. The 3D CS-Au NPs/hPPy sensing interface was tested with the highest electrochemical peak current signal shown as curve a. Then, the decreased current response signal of anti-CEA/3D CS-Au NPs/hPPy was recorded shown as curve b, which resulted from the successful fixation of anti-CEA on the surface of 3D CS-Au NPs/hPPy. The anti-CEA formed an electron barrier layer and the electron transfer was hindered. After that, the current response signal was further reduced shown as curve c after being sealed with BSA (BSA/anti-CEA/3D CS-Au NPs/hPPy) and incubating in CEA solution (CEA/BSA/anti-CEA/3D CS-Au NPs/hPPy) shown as curve d, which resulted from the further inhibition of electron transfer by the insulating protein layer. The experimental results reflected that the immunosensor was successfully construted layer by layer. The Nyquist diagrams representing the electrochemical impedance spectrum of the immunosensor were shown in Fig. 3B. The impedance diagram of 3D CS-Au NPs/hPPy sensing interface (curve a) showed a small semicircle, indicating that

3D CS-Au NPs/hPPy sensor had a lower charge transfer impedance in electrolyte solution. The curve b showed that the resistance increase slightly when anti-CEA was successfully fixed on the interface of 3D CS-Au NPs/hPPy. Following that, the resistance of BSA/anti-CEA/3D CS-Au NPs/hPPy (curve c) increased compared with that of anti-CEA/3D CS-Au NPs/hPPy, indicating that BSA was successfully modified. When CEA was successfully modified, the diameter of the semicircle region of Nyquist curve was the largest (curve d), which proved again that the complex produced by immune reaction had poor conductivity and further hindered electron transfer. It could be seen that the electron transfer rate decreased with the construction of immunosensor, which were consistent with that of the CV electrochemical detection.

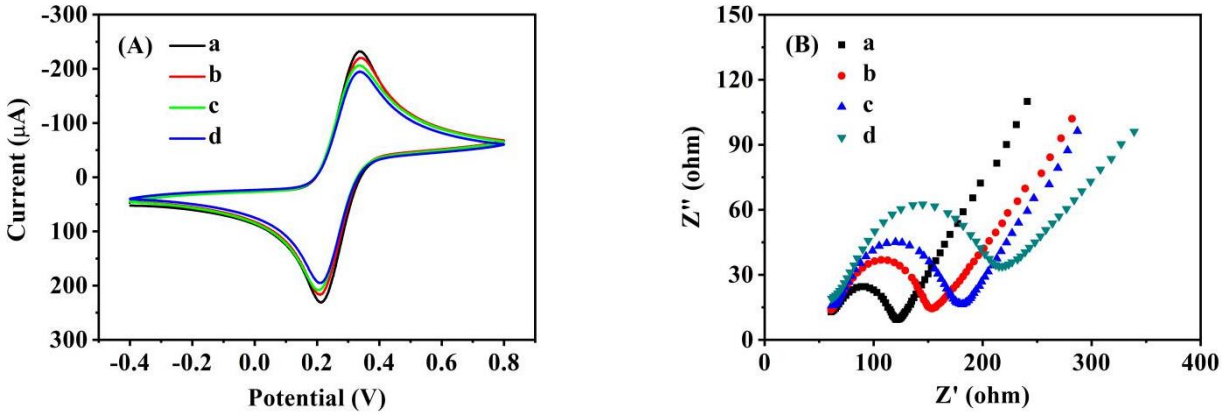

Figure 3. (A) CV diagrams of (a) 3D CS-Au NPs/hPPy, (b) anti-CEA/3D CS-Au NPs/hPPy, (c)BSA/anti-CEA/3D CS-Au NPs/hPPy, (d) CEA/BSA/anti-CEA/3D CS-Au NPs/hPPy. Scan rate: 0.1 V/s (B) EIS diagrams matching with (A). All tests were performed in 0.1 M PBS (pH 7.0) solution containing 0.1 M KCl and 10 mM $Fe(CN)_6^{3-}/Fe(CN)_6^{4-}$.

3.3. Optimization of detection conditions

The inappropriate pH value may lead to protein denaturation, which makes the activity of antigen and antibody as well as the affinity between them affected by different pH values of solution. The prepared sensor was placed in PBS buffer solution with varied pH values for detection. The relationship betwee peak current and pH of detecting 60 ng/mL CEA by DPV was obtained in Fig. 4. The results showed that in the pH range from 5.5 to 8.5, the greater the pH, the higher the peak current. When the pH value exceeded 7.0, the peak current decreased with the increase of pH. It may be the reason that the activity and stability of protein will be damaged by highly acidic or alkaline environment. Therefore, the optimal pH value of CEA detection was 7.0, which was consistent with the optimal pH used by Lan et al. [23] and Kong et al. [31].

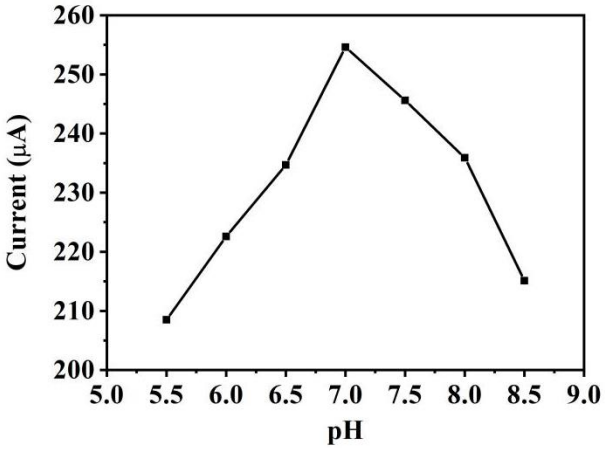

Figure 4. Influence of different pH values on peak current with the 0.1 M PBS solution containing 0.1 M KCl and 10 mM $Fe(CN)_6^{3-}/Fe(CN)_6^{4-}$ at scan rate of 0.1 V/s.

The incubation time was another significant variable affecting the electrochemical behavior of immunosensors. The DPV detection was conducted after incubating BSA/anti-CEA/3D CS-Au NPs/hPPy material with certain concentration CEA for 10, 20, 30, 40, 50, 60, 90 and 120 minutes shown as Fig. 5. The variation of peak current with incubation time was obtained in Fig. 5. With the enhancement of incubation time, the current response fell off, which could attribute to the formation of complexes in immune response. After 40 minutes, the peak current tended to be stable, so the following experiments select 40 minutes as the incubation time. 40 min was also selected by Lan et al. [23], Cao et al. [32] and Yang et al. [33] as optimal incubation period with CEA.

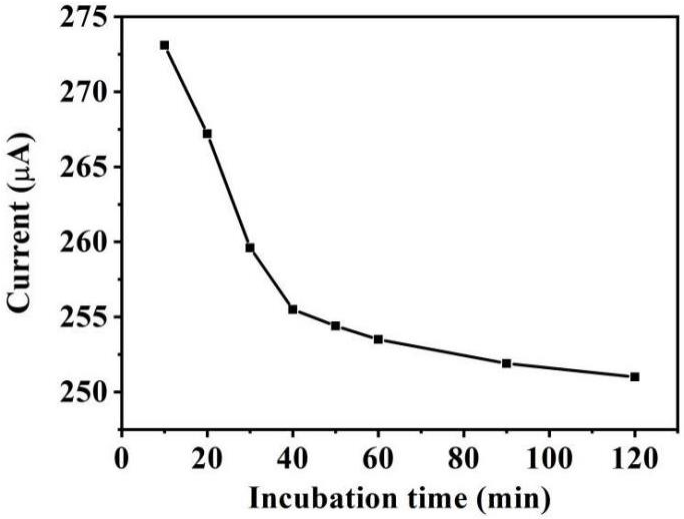

Figure 5. Variation of incubation time with peak current with the 0.1 M PBS (pH 7.0) solution containing 0.1 M KCl and 10 mM $Fe(CN)_6^{3-}/Fe(CN)_6^{4-}$ at scan rate of 0.1 V/s.

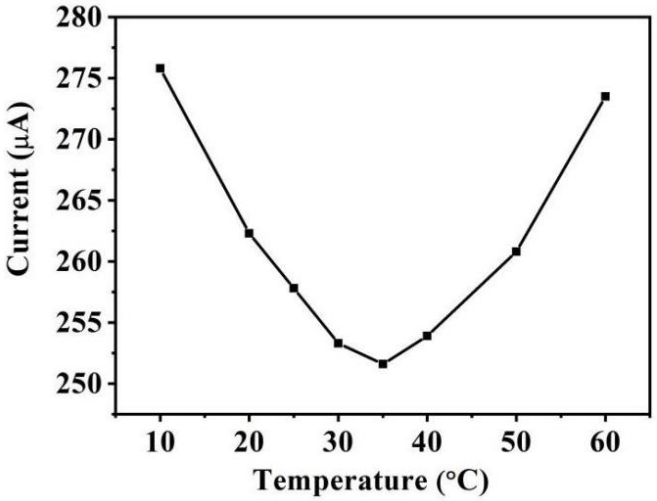

Figure 6. Variation of incubation temperature on peak current with the 0.1 M PBS (pH 7.0) solution containing 0.1 M KCl and 10 mM $Fe(CN)_6^{3-}/Fe(CN)_6^{4-}$ at scan rate of 0.1 V/s.

The efficiency of specific recognition between antigen and antibody was affected by the temperature of immune reaction, which made the electrical response depends largely on the incubation temperature. Therefore, the temperature range of 10 ℃ to 60 ℃ was choosen for immune reaction with 60 ng/mL CEA. As shown in Fig. 6, it was observed that the current response decreased with the temperature rising from 10℃ to 35℃, and then increased with the temperature rising above 35 ℃. It could ascribe to the fact that the immune complexs formed gradually when the temperature increased from 10 ℃ to 35 ℃, which resulted in suppressed current response of immunosensor. However, when the incubation temperature was higher than 35 ℃, the irreversible denaturation of CEA and anti-CEA related to the process could be caused. All datas indicated that 35 ℃ was the best temperature for immune reaction. However, in consideration of the activity of biomolecules and the lifetime of sensor, 37 ℃ was chosen as the optimal incubation temperature for practical application. The same incubation temperature was adopted by Li et al. [34] for deceting CEA.

3.4. Quantitative detection of CEA by DPV

In order to evaluate the capability of the immunosensor, based on the optimal experiemntal conditions, the electrochemical performance of the immunosensor at different standard concentrations of antigen was studied, and the relationship between the antigen concentration and the response current of the immunosensor was obtained. The DPV curves under different concentrations of CEA from 0.01 to 120 ng/mL were obtained shown as Fig. 7A. The results showed that the DPV peak current measured by immunosensor fell off with the enhancement of CEA concentration, which could be attributed to the fact that more CEA could bind fixed antibody in higher concentration of antigen solution, and the complex became a kinetic barrier for the electron transfer of ferricyanide.

The calibration curve of detecting CEA with the constructed immunosensor was exhibited in Fig. 7B. The current change of 3D CS-Au NPs/hPPy based immunosensor was linearly related to the concentration of CEA ranged from 0.01 to 120 ng/mL. The linear variation could be expressed as the

regression equation, I (μA) = 283.4296-0.4832 $C_{[CEA]}$ (ng/mL), with the correlation coefficient (R^2) of 0.9981 and the detection limit of 0.0036 ng/mL (S/N = 3). The performance of the immunosensor prepared in this work to detect CEA was in contrast to other methods as shown in table 1. The immunosensor we prepared revealed excellent capability with wide detection range and low detection limit.

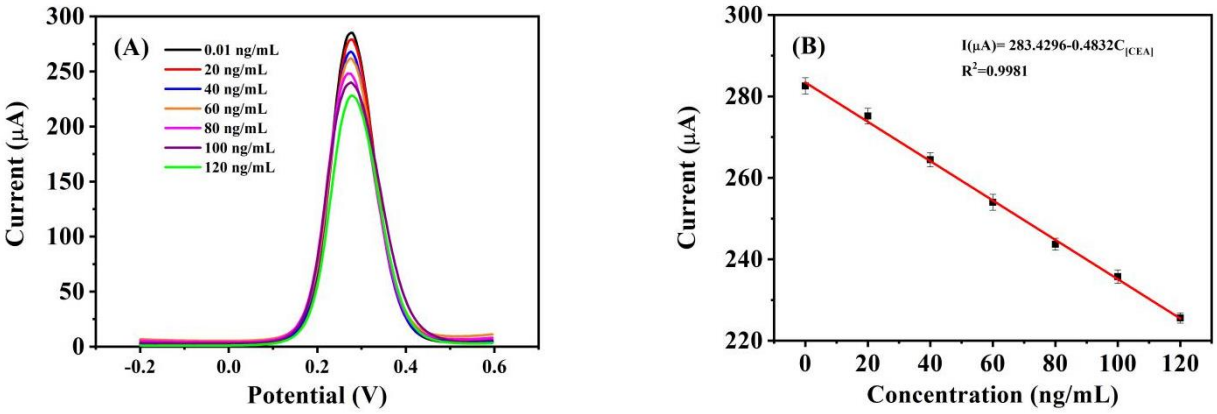

Figure 7. (A) The DPV curves of BSA/anti-CEA/3D CS-Au NPs/hPPy with different concentrations of CEA; (B) The calibration curves for the analysis different concentrations of CEA. All tests were performed in 0.1 M PBS (pH 7.0) solution containing 0.1 M KCl and 10 mM $Fe(CN)_6^{3-}$ /$Fe(CN)_6^{4-}$ at scan rate of 0.1 V/s.

Table 1. Comparison of CEA detection with varied methods

methods[a]	material	linear range	LOD	refs
ELISA	microwell plate	0.5-80 ng/mL	0.5 ng/mL	14
ECL	ZnS-CdS/MoS_2	0.05-20 ng/mL	0.031 ng/mL	16
CL	carbon dots	0.5-1 ng/mL	0.3 ng/mL	17
SPR	gold chip	3-400 ng/mL	3.0 ng/mL	15
EC	Pt NPs@rGo@PS NSs	0.05-70 ng/mL	0.01 ng/mL	23
EC	CGS–MB	0.5-80 ng/mL	0.05 ng/mL	31
EC	AuNPs/MB/Gp-Nf	0.5-120 ng/mL	0.17 ng/mL	34
EC	IL-rGO-Au-PDDA-PB	0.1-80 ng/mL	0.04 ng/mL	35
EC	PEDOT-PPy	100-100000 ng/mL	0.14 ng/mL	36
EC	Aminophenol	2.5-1500 ng/mL	3 ng/mL	37
EC	Apt2-AuNPs-Fc	1-200 ng/mL	0.5 ng/mL	38
EC	Thi-PSS-IL-rGO -AuNPs	0.05-100 ng/mL	0.02 ng/mL	39
EC	3D CS-Au NPs/hPPy	0.01-120 ng/mL	0.0036 ng/mL	this work

[a]ELISA, enzyme-linked immunosorbent assay; ECL, electrochemiluminescence; CL, chemiluminescence; SPR, surface plasmon resonance; EC, electrochemistry.

3.5. Anti-interference and stability of the immunosensor

For the sake of detecting the current response of the constructed immunosensor to interference or cross recognition, some probable interfering factors, such as AFP, UA, AA and Glu, were used to evalute the specificity of the immunpsensor shown as Fig. 8A. In the existence of 180 ng/mL interfering agent, the immunosensor was incubated with 60 ng/mL CEA and found that there was no obvious response signal difference between pure CEA and CEA with interfering substances shown as Fig. 8B, indicating that the immunosensor had a favorable CEA detection specificity.

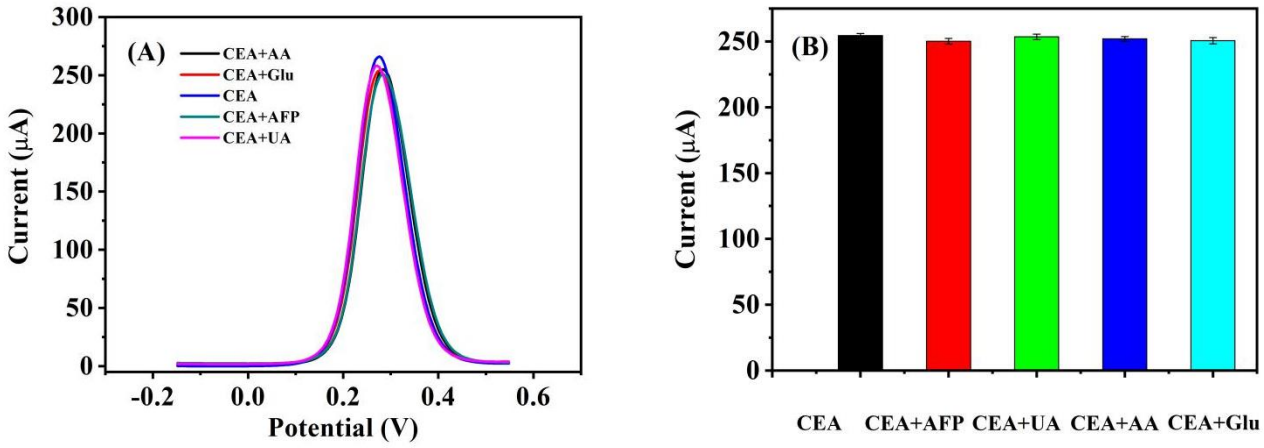

Figure 8. (A) The specificity of immunosensor for CEA, CEA+AFP, CEA+UA, CEA+AA, CEA+Glu in 0.1 M PBS (pH 7.0) solution containing 0.1 M KCl and 10 mM $Fe(CN)_6^{3-}/Fe(CN)_6^{4-}$ at scan rate of 0.1 V/s; (B) peak current matching with (A).

As shown in Fig. 9, after 50 cycles of the CEA/BSA/anti-CEA/3D CS-Au NPs/hPPy modified immunosensor, the CV detection showed almost overlapping curves, which made clear that the immunosensor had a favorable cycle stability. All datas reflected the good binding state of CEA/BSA/anti-CEA/3D CS-Au NPs/hPPy.

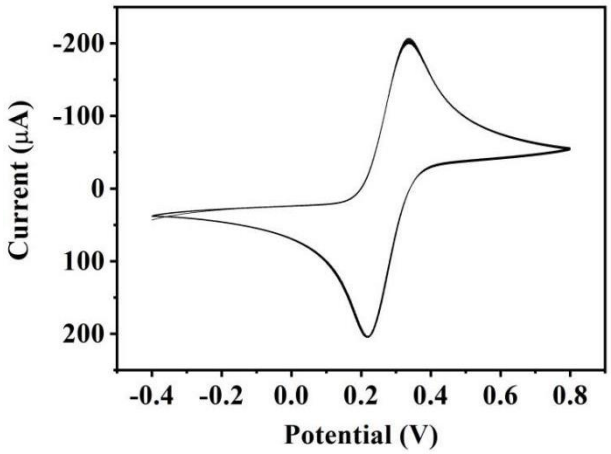

Figure 9. The CV diagram of immunosensor in 50 cycles in 0.1 M PBS (pH 7.0) solution containing 0.1 M KCl and 10 mM $Fe(CN)_6^{3-}/Fe(CN)_6^{4-}$ at scan rate of 0.1 V/s.

3.6. Real sample analysis

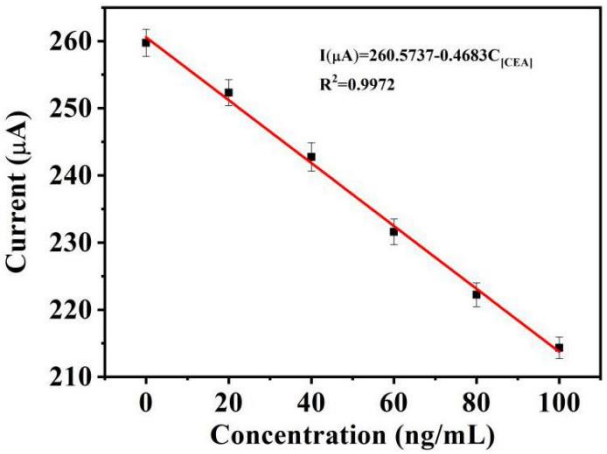

Figure 10. The calibration curves of different concentrations of CEA in human blood detected by immunosensor.

The current response equation of immunosensor to different concentrations of CEA in human blood was obtained as I(μA) = 260.5737 - 0.4683 $C_{[CEA]}$ (ng/mL) with R^2 of 0.9972 shown as Fig. 10. In order to assess the reliability and utilization potentiality of the constructed immunosensor, the results of CEA determination in human blood samples obtained by this method were in contrast to the reference values measured by the Roche electroluminescence method (RECLIA). The data listed in table 2 revealed that the datas measured by immunosensor in whole blood were basically consistent with those in serum samples detected by hospital. In addition, many components in blood were separated from serum, which would affected the actual detection results. And the datas measured in whole blood were closed to the actual value, which made the immunosensor could be used to detect CEA in whole blood.

Table 2. Comparison of detecting CEA in clinical blood samples by proposed immunosensor and RECLIA.

blood samples	our work (ng/mL)	RECLIA (ng/mL)	relative deviation(%)
1	30.00	31.55	5.167
2	15.11	15.72	4.037
3	8.72	8.62	1.147

4. CONCLUSIONS

In this work, a novel electrochemical immunosensor containing 3D CS-Au NPs/hPPy was successfully prepared. The immunosensor had been used in electrochemical detection of CEA with excellent performance including wide detection scope of 0.01 to 120 ng/mL and low detection limit of 0.0036 ng/mL. Meanwhile, the immunosensor showed good conductivity, anti-interference and stability. In addition, the immunosensor was applied to the detection of CEA in clinical human blood, and the results were basically consistent with the hospital detection, indicating that the immunosensor could be employed in determination of CEA in whole blood. In conclusion, the sensors platform we proposed will provide great help for early diagnosis and clinical treatment of related diseases, and lay a good foundation for the accurate and rapid detection of some disease markers.

ACKNOWLEDGEMENTS
This research received financial support from the university-level platform project of Suzhou University (2019ykf06, 2020ykf08) and PhD Research Funding of Suzhou University (2020BS007, 2019jb27, 2019jb23), Natural science research project of Anhui Education Department (KJ2019A0669, KJ2019A0671, KJ2020A0730), Analytical Chemistry Teaching Team(2019jxtd111).

References

1. L. K. Penny and H. M. Wallace, *Chem. Soc. Rev.,* 44 (2015) 8836.
2. M. Q. He, K. Wang, W. J. Wang, Y. L. Yu and J. H. Wang, *Anal. Chem.,* 89 (2017) 9292.
3. B. Zhao, J. Yan, D. F. Wang, Z. L. Ge, S. J. He, D. N. He, S. P. Song and C. H. Fan. *Small,* 15 (2013) 2595.
4. S. V. Staden, R. M. Ilie-Mihai, F. Pogacean and S. Pruneanu, *J. Porphyr. Phthalocya.,* 23 (2019) 1365.
5. Y. Moon, S. Y. Choi, J. K. Park and K. Y. Lee, *World. J. Surg.,*44 (2020) 1658.
6. X. Li, X. J. Zhang, Z. Wang, Q. Q. Zhang, W. X. Xuan and L. J. Ma, *Int. J. Electrochem. Sci.,* 11 (2016) 10020.
7. L. A. A. N. A. Truta and M. G. F. Sales, *Curr. Top. Med. Chem.,* 15 (2015) 256.
8. A. M. Chorcea and A. M. O. Brett, *Bioelectrochemistry,* 63 (2004) 229.
9. A. Huang, N. S. Vyas, S. E. Mercer and R. G. Phelps, *J. Cutan. Pathol.,* 46 (2019) 243.
10. Q. Han, R. Wang, B. Xing, T. Zhang, M. S. Khan, D. Wu and Q. Wei, *Biosens. Bioelectron.,* 99 (2018) 493.
11. G. F. Jie, J. J. Ge, X. S. Gao and C. L. Li, *Biosens. Bioelectron.,* 118 (2018) 115.
12. H. Medetalibeyoglu, G. Kotan, N. Atar and M. L. Yola, *Anal. Chim. Acta,* 1139 (2020) 100.
13. J. C. Kemmegne-Mbouguen, E. Ngameni, P. G. Baker, T. T. Waryo and E. I. Iwuoha, *Int. J. Electrochem. Sci.,* 9 (2014) 478.
14. S. S. Zhang, J. Yang and J. Lin, *Bioelectrochemistry,* 72 (2008) 47.
15. Z. Altintas, Y. Uludag, Y. Gurbuz and I. E. Tothill, *Talanta,* 86 (2011) 377.
16. Y. M. Liu, Y. L. Wang, J. T. Cao and Y. H. Chen, *Anal. Methods,* 8 (2016) 5242.
17. H. Miao, L. Wang, Y. Zhuo, Z. N. Zhou and X. M. Yang, *Biosens. Bioelectron.,* 86 (2016) 83.
18. A. P. M. Tavares, L. A. A. N. A. Truta, F. T. C. Moreira, L. P. T. Carneiro and M. G. F. Sales, *Biosens. Bioelectron.,* 140 (2019) 111320.

19. A. A. Jamali, M. Pourhassan-Moghaddam, J. E. N. Dolatabadi and Y. Omidi, *Trac-Trend. Anal. Chem.*, 55 (2014) 24.
20. J. F. Ping, Y. B. Zhou, Y. Y. Wu, V. Papper, S. Boujday, R. S. Marks and T. W. J. Steele, *Biosens. Bioelectron.*, 64 (2015) 373.
21. S. X. Ning, M. Q. Zhou, C. Liu, G. I. N. Waterhouse, J. Dong and S. Y. Ai, *Anal. Chim. Acta*, 1062 (2019) 87.
22. J. Zhao, Z. Z. Zhu, X. Huang, X. J. Hu and H. X. Chen, *Microchim. Acta*, 187 (2020) 231.
23. Q. C. Lan, C. L. Ren, A. Lambert, G. S. Zhang, J. Li, Q. Cheng, X. Y. Hu and Z. J. Yang, *ACS Sustainable Chem. Eng.*, 8 (2020) 4392.
24. K. C. L. Black, Z. Liu and P. B. Messersmith, *Chem. Mater.*, 23 (2011) 1130.
25. P. Gupta, A. Bharti, N. Kaur, S. Singh and N. Prabhakar, *J. Electroanal. Chem.*, 813 (2018) 102.
26. J. Li, L. Liu, Y. J. Ai, Y. Liu, H. B. Sun and Q. L. Liang, *ACS Appl. Mater. Interfaces*, 12 (2020) 5500.
27. A. Morozan, P. Jégou, S. Campidelli, S. Palacin and B. Jousselme, *Chem. Commun.*, 48 (2012) 4627.
28. J. Wang, Y. Xu, F. Yan, J. Zhu and J. Wang, *J. Power Sources*, 196 (2011) 2373.
29. Y. Bai, Y. L. Xu, J. Wang, M. Gao and J. Wang, *Acs Appl. Mater. Interfaces*, 6 (2014) 4693.
30. 30. C. Sun, L. Ma, Q. H. Qian, S. Parmar, W. B. Zhao, B. Zhao and J. Shen, *Analyst*, 139 (2014) 4216.
31. F. Y. Kong, B. Y. Xu, Y. Du, J. J. Xu and H. Y. Chen, *Chem. Commun.*, 49 (2013) 1052.
32. L. L. Cao, H. L. Xiao, C. Fang, F. J. Zhao and Z. C. Chen, *Microchim. Acta.*, 187 (2020) 584.
33. Y. X. Yang, M. Jiang, K. H. Cao, M. Wu, C. L. Zhao and H. L. Li, *Microchem. J.*, 151 (2019) 104223.
34. Y. Li, W. K. Yang, M. Q. Fan and A. Fan, *Anal. Sci.*, 27 (2011) 727.
35. Q. Gao, N. Liu and Z. Ma, *Anal. Chim. Acta*, 829 (2014) 15.
36. A. P. M. Tavares, L. A. A. N. A. Truta, F. T. C. Moreira, L. P. T. Carneiro and M. G. F. Sales, *Biosens. Bioelectron.*, 140 (2019) 111320.
37. L. A. A. N. A. Truta and M. G. F. Sales, *Sens. Actuators B Chem.*, 287 (2019) 53.
38. H. W. Shu, W. Wen, H. Y. Xiong, X. H. Zhang and S. F. Wang, *Electrochem. Commun.*, 37 (2013) 15.
39. T. Xu, J. Ma and Z. F. Ma, *New. J. Chem.*, 39 (2015) 1006.